arXiv:0710.1540v2 [hep-ph] 1 Apr 2008

Jet quenching parameter $\hat{q}$ in the stochastic QCD vacuum with Landau damping

Dmitri Antonov, Hans-Jürgen Pirner

Institut für Theoretische Physik, Universität Heidelberg,

Philosophenweg 19, D-69120 Heidelberg, Germany

We argue that the radiative energy loss of a parton traversing the quark-gluon plasma is determined by Landau damping of soft modes in the plasma. Using this idea, we calculate the jet quenching parameter of a gluon. The calculation is done in SU(3) quenched QCD within the stochastic vacuum model. At the LHC-relevant temperatures, the result depends on the gluon condensate, the vacuum correlation length, and the gluon Debye mass. Numerically, when the temperature varies from $T = T_c$ to $T = 900\,\mathrm{MeV}$, the jet quenching parameter rises from $\hat{q} = 0$ to approximately $1.8\,\mathrm{GeV}^2/\mathrm{fm}$. We compare our results with the predictions of perturbative QCD and other calculations.

I. INTRODUCTION

At RHIC and LHC energies, radiative energy loss is an important mechanism for jet energy loss in the quark-gluon plasma [1]. It is related to the mean transverse momentum $\langle p_\perp^2 \rangle$ which the parton acquires traversing the plasma. The momentum broadening of the parton is proportional to the distance it travels, therefore the integrated total energy loss from radiation due to the acceleration is proportional to the distance travelled squared $L_\parallel^2$ [1]. The energy loss is parametrized by the jet quenching parameter $\hat{q}$

$$\Delta E = \frac{\alpha_s}{8} C_R \hat{q} L_\parallel^2,$$

where C_R is the quadratic Casimir operator of the representation R of the parton, and α_s is the strong coupling constant at an appropriate scale. The jet quenching parameter can be estimated in a dilute plasma perturbatively:

$$\hat{q} = \left\langle \sigma p_\perp^2 \right\rangle \rho \propto T^3 \int \frac{d\sigma}{dp_\perp^2} p_\perp^2 d^2 p_\perp \sim \alpha_s^2 N_c^2 T^3 \ln \frac{1}{g}.$$

The perturbative temperature dependence of $\hat{q}$ is determined by the density of scattering partners $\rho \propto T^3$ and the differential transport Coulomb cross section, which is cut off in the infra-red at the Debye mass.

A standard nonperturbative calculation of the jet quenching parameter can be done with the help of the dipole formalism [2]. In this formalism, a fake dipole of size $L_\perp$ is constructed from the partons in the T-amplitude and in the T^*-amplitude, the trajectories of which are displaced from each other by the distance $L_\perp$. The transport parameter $\langle \sigma p_\perp^2 \rangle$ can then be calculated from the cross section of this fake dipole. In the dipole model, for a dipole of size $L_\perp$ one has:

$$\sigma(L_\perp) = \mathrm{tr} \int d^2b \left\langle |V(\mathbf{b}) - V(\mathbf{b}+\mathbf{L}_\perp)|^2 \right\rangle =$$

$$= \mathrm{tr} \int d^2b \left\langle 2 - V(\mathbf{b})V^\dagger(\mathbf{b}+\mathbf{L}_\perp) - V^\dagger(\mathbf{b})V(\mathbf{b}+\mathbf{L}_\perp) \right\rangle .$$

Here

$$V(\mathbf{b}) = \mathcal{P} \exp\left[igv_\mu \int_{-\infty}^{+\infty} d\tau A_\mu(x(\tau)) \right]$$

is the Wilson line of a parton with the impact parameter $\mathbf{b}$ propagating with the 4-velocity $v_\mu = (1, \mathbf{v})$, $\mathbf{v}^2 = 1$, $\mathbf{vb} = 0$, and $x(\tau) = (\tau, \mathbf{b} + \mathbf{v}\tau)$ [29]. The nonperturbative differential cross section to produce a parton with the transverse momentum $p_\perp$ is then given by Fourier transform

$$\frac{d\sigma}{dp_\perp^2} = \int d^2L_\perp \mathrm{e}^{i\mathbf{p}_\perp \mathbf{L}_\perp} \,\mathrm{tr} \int d^2b \left\langle 2 - V(\mathbf{b})V^\dagger(\mathbf{b}+\mathbf{L}_\perp) - V^\dagger(\mathbf{b})V(\mathbf{b}+\mathbf{L}_\perp) \right\rangle .$$

The expectation values $\langle \ldots \rangle$ of the Wilson lines have to be evaluated with the target ground states. The excited states are summed over. The transport parameter can then be obtained by differentiation

$$\left\langle \sigma p_\perp^2 \right\rangle =$$

$$= \int \frac{d^2p_\perp}{(2\pi)^2} \int d^2L_\perp \left(-\nabla_\perp^2 \mathrm{e}^{i\mathbf{p}_\perp \mathbf{L}_\perp} \right) \,\mathrm{tr} \int d^2b \left\langle 2 - V(\mathbf{b})V^\dagger(\mathbf{b}+\mathbf{L}_\perp) - V^\dagger(\mathbf{b})V(\mathbf{b}+\mathbf{L}_\perp) \right\rangle .$$

After a partial integration, one sees that because of the $p_\perp$-integration only the $L_\perp^2$-dependent part, i.e. the first-order term in the dipole cross section is relevant for $p_\perp$-broadening calculation. When one takes the expectation value in the medium, the density of scattering partners in the medium enters. One can replace the traced products of Wilson lines, $\mathrm{tr}\, VV^\dagger$ and $\mathrm{tr}\, V^\dagger V$, by two gauge-invariant Wilson loops, which facilitates the calculation. For

example, one has

$$\mathrm{tr}\, V(\mathbf{b})V^\dagger(\mathbf{b}+\mathbf{L}_\perp) = \mathrm{tr}\,\mathcal{P}\exp\left\{igv_\mu\int_{-\infty}^{+\infty} d\tau\,[A_\mu(x(\tau)) - A_\mu(y(\tau))]\right\},$$

where $y(\tau) = (\tau, \mathbf{b}+\mathbf{L}_\perp - \mathbf{v}\tau)$. One can approximate two long parallel lines $x(\tau)$ and $y(\tau)$ by a contour, which closes asymptotically at $\tau = \pm\infty$, where the interactions vanish. This yields the Wilson loop

$$\mathrm{tr}\, V(\mathbf{b})V^\dagger(\mathbf{b}+\mathbf{L}_\perp) \simeq \mathrm{tr}\,\mathcal{P}\exp\left[ig\int_0^1 ds\dot{z}_\mu(s)A_\mu(z(s))\right]$$

defined at the united contour

$$z_\mu(s) = \begin{cases} x_\mu(\tau(s)), & s\in\left(0,\frac{1}{2}\right) \\ y_\mu(\tau(s)), & s\in\left(\frac{1}{2},1\right)\end{cases}, \quad \text{where} \quad \tau(s) = \tan(2\pi(s-1/4)).$$

At high energies, the S-matrix for dipole scattering is mostly real-valued because of purely absorptive interactions (Pomeron exchange). Other contributions have been discussed in the literature [3, 4]. In the calculation, which we will present in this paper, the S-matrix has both real- and imaginary-valued parts, therefore we have to guarantee the reality of the cross section by using the real-valued part of the expectation value of the Wilson loop. The real-valued part of the expectation value of the Wilson loop in the medium can be related to the transport parameter $\hat{q}$ as follows (see e.g. Ref. [5]):

$$\left\langle \mathrm{Re}\, W^{\mathrm{Mink}}_{L_\parallel\times L_\perp}\right\rangle = \exp\left(-\frac{\hat{q}}{4\sqrt{2}}L_\parallel L_\perp^2\right). \tag{1}$$

As a tool to obtain the Wilson-loop expectation value we will use the so-called stochastic vacuum model (SVM) [6] in Minkowski space-time. This model has been applied to high energy hadron-proton and γ^*-proton scattering [7] with two Wilson loops representing projectile and target particles. Recently, a single Wilson loop near the light cone has also been studied within the SVM in Ref. [8]. This calculation is tricky since the expectation value of the Wilson loop on the light cone is strictly zero in vacuum, the limiting procedure of approaching the light cone, however, can give the quark-antiquark confining interaction in the light-cone Hamiltonian.

In Fig. 1 we show the arrangement which we use for the following calculation. The long side of the contour of the Wilson loop is directed along the light cone. The mean $\langle p_\perp^2\rangle$ is related to the transverse size $L_\perp$ of the contour. A counterintuitive property of

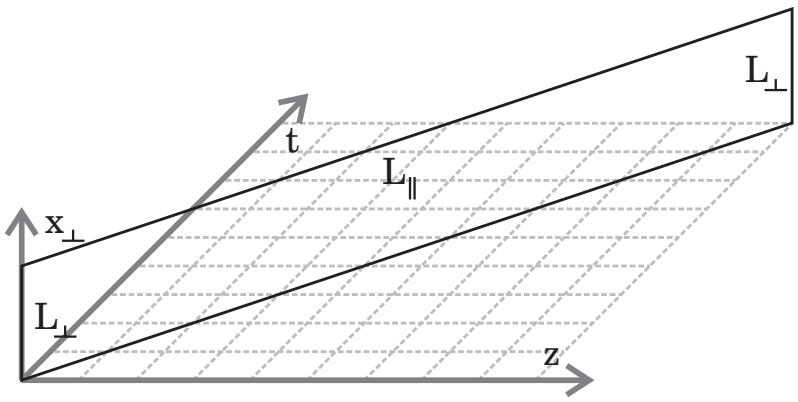


Figure 1: The contour of the Wilson loop ($L_{\parallel} \times L_{\perp}$) of a gluon.

Eq. (1) is its exponential fall-off, since normally an expectation value of a Wilson loop in Minkowski space-time contains the imaginary unity i in the argument of the exponent [8]. We will demonstrate that the exponential fall-off is a consequence of Landau damping of soft modes in the quark-gluon plasma and calculate through this mechanism the jet quenching parameter $\hat{q}$.

Recently, a calculation of $\hat{q}$ at strong coupling has been done for $\mathcal{N} = 4$ SYM in Refs. [5], with the help of the AdS/CFT-correspondence. It yields $\hat{q} \propto T^3$, which is a consequence of conformal invariance. However, it may be that at LHC-relevant temperatures, the QCD conformal anomaly still plays an important role. Lattice results on $(\varepsilon - 3p) \neq 0$ indicate that the energy density ε and the pressure p deviate from pure Stefan-Boltzmann behavior. For this reason, one may expect a violation of conformal invariance and an explicit dependence of $\hat{q}$ on the gluon condensate, which arises in the SVM. Of course, the chromo-electric gluon condensate vanished at high temperatures after deconfinement, but there can remain a chromo-magnetic condensate, and nonvanishing correlations between chromo-magnetic field strengths in the quark-gluon plasma. One of our main objectives in this paper is to investigate their effect on the jet quenching parameter $\hat{q}$.

The paper is organized as follows. In section II, we review some basics about the SVM at $T = 0$ and $T > T_c$. We also introduce there an effective local formulation of the SVM, which will be technically important for the subsequent analysis. In section III, we incorporate Landau damping into the model and calculate the jet quenching parameter. In section IV we summarize the main results of the paper.

II. GENERALITIES ON WILSON LOOPS AND THE SVM

We start considering the expectation value of a Wilson loop in Euclidean space-time at zero temperature ($T = 0$). In an arbitrary representation R of $\mathrm{SU}(N_c)$, it reads $\Big\langle W(C) \Big\rangle \equiv \Big\langle \mathrm{tr}\, \mathcal{P} \exp\Big(ig \oint\limits_C dx_\mu A_\mu \Big) \Big\rangle$. In the SVM, one uses the non-Abelian Stokes' theorem and the cumulant expansion to write the Wilson-loop average as follows [6]:

$$\Big\langle W(C) \Big\rangle \simeq \mathrm{tr}\, \exp\left[-\frac{1}{2!} \frac{g^2}{4} \int\limits_{\Sigma(C)} d\sigma_{\mu\nu}(x) \int\limits_{\Sigma(C)} d\sigma_{\lambda\rho}(x') \left\langle F_{\mu\nu}(x) F_{\lambda\rho}(x') \right\rangle \right]. \tag{2}$$

Here, $\Sigma(C)$ is the surface encircled by the flat contour C. Averages involving gluonic field strengths are calculated in the SVM by using the two-point correlation function $\langle F_{\mu\nu}(x) F_{\lambda\rho}(x') \rangle$, which has been fitted to lattice data [9]. To simplify notations, we suppress two phase factors between the points x and x' in the fundamental representation. Fixing the Fock-Schwinger gauge with the reference point in either of these two points, one can see that these phase factors are anyhow equal to $\hat{1}_R$ when the path between the points x and x' is the straight line. The approximate equality in Eq. (2) is due to the use of the cumulant expansion, which gives the correct area law for the heavy quark-antiquark Wilson loop. It is supported by lattice data [10]-[14] and states that the amplitude of the two-point irreducible gauge-invariant correlation function (cumulant) of $F_{\mu\nu}$'s dominates over the amplitudes of higher-order cumulants, which are therefore neglected. The factor 1/2! in Eq. (2) is due to the cumulant expansion, and the factor 1/4 is due to the non-Abelian Stokes' theorem.

Within the SVM, one parametrizes the nonperturbative part of the two-point cumulant as follows [6, 15]:

$$\begin{aligned} \left\langle F^a_{\mu\nu}(x) F^b_{\lambda\rho}(x') \right\rangle = \delta^{ab} \frac{\left\langle (F^a_{\mu\nu})^2 \right\rangle}{12(N_c^2 - 1)} \Bigg\{ & \kappa (\delta_{\mu\lambda}\delta_{\nu\rho} - \delta_{\mu\rho}\delta_{\nu\lambda}) D(u^2) + \\ & + \frac{1-\kappa}{2} \left[\partial_\mu \left(u_\lambda \delta_{\nu\rho} - u_\rho \delta_{\nu\lambda} \right) + \partial_\nu \left(u_\rho \delta_{\mu\lambda} - u_\lambda \delta_{\mu\rho} \right) \right] D_1(u^2) \Bigg\}. \end{aligned} \tag{3}$$

Here, D and D_1 are dimensionless functions of the distance $u = x - x'$ normalized by the condition $D(0) = D_1(0) = 1$. The gluon condensate defines the amplitude of this correlation function. The function D is responsible for the confining properties of the non-Abelian gauge theory. The function D_1 describes Abelian-like self-interactions of the Wilson loop, which do not lead to an expectation value of the form of Eq. (1). High-energy scattering data yield

$\kappa = 0.74$ in the vacuum [15]. We will take $\kappa = 1$, i.e. disregard the small contribution of the function D_1 altogether. Lattice simulations [10]-[14] yield an exponential fall-off of the function D:

$$D(u^2) = \mathrm{e}^{-\mu|u|}$$

with the inverse vacuum correlation length [12]

$$\mu = 894\,\mathrm{MeV}.$$

One can rewrite the Wilson-loop average using the the surface tensor

$$\Sigma_{\mu\nu}(x) = \int_{\Sigma(C)} d\sigma_{\mu\nu}(w(\xi))\delta(x - w(\xi)).$$

The two-dimensional vector $\xi = (\xi_1, \xi_2)$, where $\xi_{1,2} \in [0, 1]$, parametrizes differential elements $d\sigma_{\mu\nu}$ on the surface $\Sigma(C)$, and $w_\mu(\xi)$ points towards each differential surface element. Using the correlation function D one obtains the characteristic form of the Wilson-loop average:

$$\Big\langle W(C) \Big\rangle \simeq \exp\left[-\frac{C_R}{48(N_c^2 - 1)} \cdot g^2 \left\langle (F_{\mu\nu}^a)^2 \right\rangle \int d^4x \int d^4y \Sigma_{\mu\nu}(x) \mathrm{e}^{-\mu|x-y|} \Sigma_{\mu\nu}(y) \right]. \quad (4)$$

In particular, for a contour C whose temporal extension is much larger than its spatial extension, one obtains an area law depending on the string tension in the fundamental representation [15, 16]

$$\sigma = \frac{\pi C_F}{12(N_c^2 - 1)} \frac{g^2 \left\langle (F_{\mu\nu}^a)^2 \right\rangle}{\mu^2} \quad \text{with} \quad C_F = \frac{N_c^2 - 1}{2N_c}. \quad (5)$$

For $N_c = 3$, we take the standard value of the string tension $\sigma = (440\,\mathrm{MeV})^2$ to estimate the gluon condensate $g^2 \left\langle (F_{\mu\nu}^a)^2 \right\rangle \simeq 3.55\,\mathrm{GeV}^4$.

We see from Eq. (4) that the SVM essentially suggests a representation of the Wilson-loop average in terms of an effective local field theory of the field strength tensor $F_{\mu\nu}^a$:

$$\Big\langle W(C) \Big\rangle = \mathrm{tr} \int \mathcal{D} F_{\mu\nu}^a \mathrm{e}^{-S_{\mathrm{Eucl}}[F]} \quad (6)$$

with the action

$$S_{\mathrm{Eucl}}[F] = \frac{1}{2} \int d^4x \left[F_{\mu\nu}^a \mathcal{K}(x) F_{\mu\nu}^a + i F_{\mu\nu}^a t^a \Sigma_{\mu\nu} \right]. \quad (7)$$

Here, $\mathcal{K}$ is a well-defined local operator, which reproduces Eq. (4) after the Gaussian integration in Eq. (6):

$$\Big\langle W(C) \Big\rangle = \exp\left[-\frac{C_R}{8} \int d^4x \int d^4y \Sigma_{\mu\nu}(x) \mathcal{K}^{-1}(x - y) \Sigma_{\mu\nu}(y) \right], \quad (8)$$

where $\mathcal{K}^{-1}(x)$ is a Green function of the operator $\mathcal{K}$: $\mathcal{K}\mathcal{K}^{-1} = \delta(x)$. Comparing Eqs. (4) and (8), we find that the kernel $\mathcal{K}^{-1}$ has an exponential fall-off:

$$\mathcal{K}^{-1}(x) = \frac{g^2 \left\langle (F^a_{\mu\nu})^2 \right\rangle}{6(N_c^2-1)} \mathrm{e}^{-\mu|x|}. \tag{9}$$

The operator $\mathcal{K}$ itself can then be obtained through Fourier transformation. In the coordinate representation, it reads

$$\mathcal{K}(x) = \frac{N_c^2-1}{2\pi^2} \frac{\mu^4}{g^2 \left\langle (F^a_{\mu\nu})^2 \right\rangle} \left(1 - \frac{\partial^2}{\mu^2}\right)^{5/2}. \tag{10}$$

At finite temperature ($T \neq 0$), the $O(4)$ space-time symmetry is broken down to the spatial $O(3)$ symmetry, and the correlation function (3) splits into the following three functions

$$\left\langle E^a_i(x) E^b_k(x') \right\rangle, \quad \left\langle E^a_i(x) B^b_k(x') \right\rangle, \quad \left\langle B^a_i(x) B^b_k(x') \right\rangle,$$

which were simulated on the lattice in Refs. [11, 12]. In the deconfined phase ($T > T_c$), the chromo-electric condensate vanishes, and so does the correlation function $\left\langle E^a_i(x) E^b_k(x') \right\rangle$. Furthermore, the amplitude of the mixed electric-magnetic correlation function is by an order of magnitude smaller than the amplitude of the magnetic-magnetic correlation function [11]. For this reason, we disregard the correlation function $\left\langle E^a_i(x) B^b_k(x') \right\rangle$ with respect to the function $\left\langle B^a_i(x) B^b_k(x') \right\rangle$, which can be parametrized as follows [30]:

$$\left\langle B^a_i(x) B^b_k(x') \right\rangle = \frac{\left\langle (F^a_{\mu\nu})^2 \right\rangle_T}{12(N_c^2-1)} \delta^{ab} \delta_{ik} D^B(u^2), \tag{11}$$

$$D^B(u^2) = \mathrm{e}^{-\mu(T)|u|}. \tag{12}$$

The temperature dependencies of the gluon condensate and of the inverse vacuum correlation length will be discussed in the next section.

III. EVALUATION OF $\hat{q}$ THROUGH LANDAU DAMPING

We want to calculate now the Wilson-loop average in the gluon plasma, i.e. in a thermal environment. At finite temperature, in the Euclidean space-time, the contour of the loop has the orientation shown in Fig. 1, namely it is oriented at 45° in the (x_4, x_3)-plane. Due to the x_4-periodicity, the contour $C = L_\parallel \times L_\perp$ effectively splits into pieces, whose extensions along

the 3rd and the 4th axes are $\beta \equiv 1/T$. Such pieces will be referred to as strips. A point lying on the surface of the strip closest to the origin can be parametrized by a vector-function

$$w_\mu(\xi_1, \xi_2) = \beta\xi_1 t_\mu + L_\perp \xi_2 r_\mu, \tag{13}$$

$$t_\mu = (0,0,1,1),\ r_\mu = (1,0,0,0),\ \xi_{1,2} \in [0,1].$$

Since we have argued to disregard the mixed correlator, only the contribution of the chromomagnetic field to the effective action should be taken into account, which yields [cf. Eq. (7)]

$$S_{\rm Eucl}[B] = \int d^4x \left(B_2^a \mathcal{K} B_2^a + i B_2^a t^a \Sigma_{13}\right). \tag{14}$$

The Wilson-loop average of one strip reads

$$\left\langle W^{\rm Eucl}_{1-{\rm strip}} \right\rangle = {\rm tr} \int \mathcal{D}B_2^a {\rm e}^{-S_{\rm Eucl}[B]} = \exp\left[-\frac{C_R}{4}\int d^4x \int d^4y \Sigma_{13}(x)\mathcal{K}^{-1}(x-y)\Sigma_{13}(y)\right]. \tag{15}$$

Note that, for $\mathcal{K}^{-1}$ given by Eq. (9), this result indeed agrees with the one following from a direct application of the cumulant expansion,

$$\left\langle W^{\rm Eucl}_{1-{\rm strip}} \right\rangle = {\rm tr}\left\langle \exp\left(i\int d\sigma_{13} B_2^a t^a\right)\right\rangle \simeq$$

$$\simeq {\rm tr}\ \exp\left[-\frac{g^2}{2}\int d\sigma_{13}(w)\int d\sigma_{13}(w') t^a t^b \left\langle B_2^a(w) B_2^b(w')\right\rangle\right],$$

when one uses $\left\langle B_2^a(w) B_2^b(w')\right\rangle$ in the form of Eq. (11).

In the full Wilson-loop average $\left\langle W^{\rm Eucl}_{L_\parallel \times L_\perp}\right\rangle$, also interactions between different strips take place besides self-interactions of one strip. Let χ_k denote the interaction between two strips separated from each other by the distance βk:

$$\chi_k = \frac{C_R}{4}\int d\sigma_{13}(w)\int d\sigma_{13}(w')\mathcal{K}^{-1}(w-w'),$$

where $w'_\mu = w_\mu(\xi'_1, \xi'_2) + (0,0,\beta k, 0)_\mu$. Here, the relative distance between the points, $|\Delta w(k)| \equiv |w - w'|$, is

$$|\Delta w(k)| =$$

$$= \left\{\left[\beta(\xi'_1 - \xi_1) + k\beta\right]^2 + \left[\beta(\xi'_1 - \xi_1)\right]^2 + \mathcal{O}\left[L_\perp^2(\xi'_2 - \xi_2)^2\right]\right\}^{1/2} \simeq \beta\sqrt{k^2 + 2kx + 2x^2}, \tag{16}$$

$$x \equiv \xi'_1 - \xi_1, \quad x \in [-1, 1].$$

In the final form of Eq. (16), we disregard $\mathcal{O}\left[L_\perp^2(\xi_2'-\xi_2)^2\right]$, since $L_\perp \ll \beta$. If this term had been retained, the final result for $\hat{q}$ would depend on the size of the color dipole, $L_\perp$. The full number of strips (i.e. the maximal value of k) is

$$n \equiv \frac{L_\parallel}{\beta\sqrt{2}}. \tag{17}$$

Therefore, the overall contribution to the Wilson-loop average reads

$$-\ln\left\langle W^{\rm Eucl}_{L_\parallel\times L_\perp}\right\rangle = \sum_{i=0}^{n-1}\sum_{k=0}^{i}\chi_k = \sum_{k=0}^{n-1}(n-k)\chi_k. \tag{18}$$

For the transport parameter $\hat{q}$ we need a calculation of the real-valued part of the adjoint Wilson-loop expectation value in Minkowski space-time. We would like to discuss this expectation value first, before we make the analytic continuation. In Minkowski space-time, in general $\left\langle W^{\rm Mink}(C)\right\rangle = \eta {\rm e}^{2i\delta}$. If one interpretes the Wilson loop as an interaction of the fake dipole with the medium, then there can be two medium effects. The fake-meson interaction can generate real- and imaginary-valued parts of the S-matrix. Absorptive effects [cf. Eq. (1)], namely the reduction of the intensity of the beam when it traverses the medium, are described by η. In addition, there is real-valued phase shift δ of the wave-function of the projectile, which it acquires propagating through the target. In our calculation, both terms will be present, but only η will contribute to $\langle\sigma p_\perp^2\rangle$. That is because the real-valued part of the S-matrix $\propto\cos(2\delta)$ differentiated twice with respect to the dipole size $L_\perp$ and evaluated then at $L_\perp = 0$ vanishes. With these preliminaries in mind we can now make the important analytic continuation to Minkowski space-time. In Minkowski space-time, the action (14) goes over to

$$S_{\rm Mink}[B] = i\int d^4x\left(B_2^a\mathcal{K}B_2^a + B_2^a t^a\Sigma_{13}\right), \tag{19}$$

and Eq. (15) becomes

$$\left\langle {\rm Re}\, W^{\rm Mink}_{\rm 1-strip}\right\rangle = {\rm tr}\,{\rm Re}\int\mathcal{D}B_2^a{\rm e}^{-S_{\rm Mink}[B]} =$$

$$= {\rm Re}\,\exp\left[i\frac{C_R}{4}\int d^4x\int d^4y\Sigma_{13}(x)\mathcal{K}^{-1}(x-y)\Sigma_{13}(y)\right]. \tag{20}$$

Until now, this average does not have an exponential fall-off. The exponential fall-off only appears when we take into account the scattering partners in the medium as external sources. The correlation functions must mediate an interaction with the gluons in the heat bath, otherwise there is no absorptive scattering. These gluons can be summed over, see Fig. 2.

They will then appear as a gluon polarization insertion into the correlation function of the field strengths. The imaginary-valued part of this polarization operator comes from the on-shell gluons in the intermediate state, which contribute to the absorptive phase. Since the imaginary-valued part of the gluon self-energy is related to the soft modes of the quark-gluon plasma [17], one sees that the energy loss is essentially linked to Landau damping of gluons. The soft background gluons with energies $\omega \equiv |p_0| \ll |\mathbf{p}|$, parametrized by the SVM correlation function, can be absorbed by thermal gluons, i.e. gluons from the thermal bath. Accordingly, the stochastic QCD vacuum becomes modified in a way, which is not accessible in Euclidean simulations on the lattice and, therefore, is not encoded in the parametrization of the D^B-function, Eq. (12). The imaginary part of the thermal loop for the gluon self-energy reads in the hard-loop approximation [17, 18]

$$\text{Im } \Pi_{ij}(\omega, \mathbf{p}) = -\pi m_D^2 \omega \int \frac{d\Omega}{4\pi} n_i n_j \delta(\omega - \mathbf{np}) =$$

$$= -\frac{\pi m_D^2 \omega}{2|\mathbf{p}|} \left[\frac{\omega^2}{\mathbf{p}^2} \cdot \frac{p_i p_j}{\mathbf{p}^2} + \frac{1}{2} \left(1 - \frac{\omega^2}{\mathbf{p}^2} \right) \cdot \left(\delta_{ij} - \frac{p_i p_j}{\mathbf{p}^2} \right) \right]. \tag{21}$$

Here $m_D = gT\sqrt{N_c/3}$ is the Debye mass of the hard thermal gluon in quenched QCD under study. The separation of the momentum scales of the correlation function and the thermal gluons is rather subtle. The correlation function contains spatial momenta of order μ, but very small energies $\omega \ll m_D$, whereas the thermal heat bath contains gluons with energies and spatial momenta of order T. For ultrasoft space-like gluons with $\omega^2 \ll \mathbf{p}^2$, only the transverse part of Eq. (21) survives:

$$\text{Im } \Pi_{ij}(\omega, \mathbf{p}) \to \left(p_i p_j - \mathbf{p}^2 \delta_{ij} \right) \cdot \mathcal{P}(\omega, \mathbf{p}),$$

$$\mathcal{P}(\omega, \mathbf{p}) = \frac{\pi m_D^2 \omega}{4|\mathbf{p}|^3}. \tag{22}$$

The linear component of the field-strength tensor ($\sim \partial_i A_j^a$) satisfies the relation

$$F_{ij}^{a\,(\text{lin})}(\mathbf{p}) F_{ij}^{b\,(\text{lin})}(-\mathbf{p}) = 2 \left(\mathbf{p}^2 \delta_{ij} - p_i p_j \right) A_i^a(\mathbf{p}) A_j^b(-\mathbf{p}).$$

Polyakov [19] has argued that, in the course of integration over hard modes, the cubic ($\sim A^3$) and the quartic ($\sim A^4$) terms appear in such a way that they supplement the square of the field-strength tensor to the standard non-Abelian form. For this reason, the spatial part of the effective action (7) in Minkowski space-time may be modified by Im $\Pi_{ij}(\omega, \mathbf{p})$:

$$S_{\text{Mink}}[F] = \frac{i}{2} \int d^4x \left[F_{ij}^a \mathcal{K}(x) F_{ij}^a + F_{ij}^a t^a \Sigma_{ij} \right] \to$$

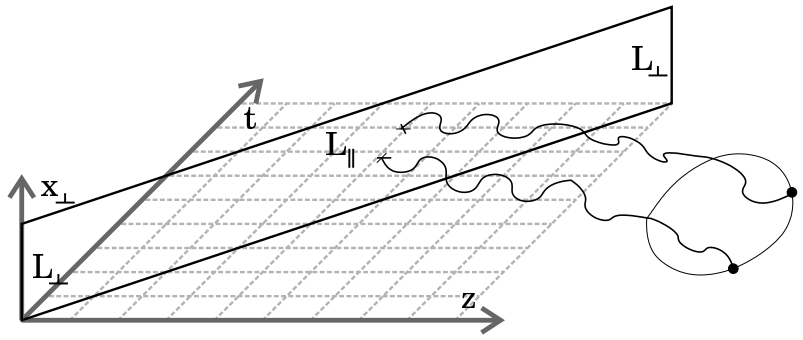


Figure 2: The Wilson-loop surface interacting with the hard gluons (drawn curve) through the soft ones (wavy curves). The imaginary part of the soft-gluon polarization operator corresponds to Landau damping. For simplicity, the splitting of the surface into strips is not depicted.

$$\to \frac{i}{2}\int d^4x \left\{F^a_{ij}\left[\mathcal{K}(x)-i\mathcal{P}(x)\right]F^a_{ij}+F^a_{ij}t^a\Sigma_{ij}\right\}. \tag{23}$$

Accordingly, Eq. (20) changes as

$$\left\langle \mathrm{Re}\, W^{\mathrm{Mink}}_{1-\mathrm{strip}}\right\rangle = \mathrm{Re}\,\exp\left[i\frac{C_R}{4}\int d^4x\int d^4y\Sigma_{13}(x)\left(\frac{1}{\mathcal{K}-i\mathcal{P}}\right)_{xy}\Sigma_{13}(y)\right]=$$

$$=\mathrm{Re}\,\exp\left[-\frac{C_R}{4}\int d^4x\int d^4y\Sigma_{13}(x)\left(\frac{\mathcal{P}-i\mathcal{K}}{\mathcal{K}^2+\mathcal{P}^2}\right)_{xy}\Sigma_{13}(y)\right]. \tag{24}$$

As was discussed, the term proportional to $i\mathcal{K}$ in Eq. (24) describes the non-absorptive part of the interaction between the fake dipole and the medium. It does not contribute to $\hat{q}$ and will henceforth be disregarded. The remaining real-valued part of Eq. (24) describes jet quenching. The interaction of the Wilson-loop surface with the hard gluons is depicted in Fig. 2. There, the closed line is the hard thermal loop, and the wavy lines are soft gluons, which mediate the interactions. The chromo-magnetic condensate and the hard gluons represent soft and hard components coexisting in the gluon plasma.

To handle the complicated Eqs. (23) and (24), we have approximated $\mathcal{P}(\omega,\mathbf{p})$ by a function $\mathcal{P}(p)$ of the full 4-momentum in the following way [31]. We denote $\omega=\zeta|\mathbf{p}|$, where $\zeta\ll 1$. Then $|\mathbf{p}|=\sqrt{\frac{-p^2}{1-\zeta^2}}$, and we have

$$\mathcal{P}(p)=-\frac{M^2(T)}{p^2},$$

$$M^2(T)\equiv\frac{\pi\zeta(1-\zeta^2)}{4}m_D^2(T). \tag{25}$$

An important property of the SVM for high-energy scattering in Minkowski space-time [7, 15] is the same exponential fall-off with transverse distance of the surface-surface correlations as in the Euclidean space-time [cf. Eq. (20)]. For this reason, one may calculate the operator $\left(\frac{\mathcal{P}}{\mathcal{K}^2+\mathcal{P}^2}\right)_{xy}$ of interest in the Euclidean space-time, where $\mathcal{P}(p) = \frac{M^2(T)}{p^2}$ and, according to Eq. (10),

$$\mathcal{K}^{-2}(p) = \frac{\mathcal{N}(T)}{[p^2+\mu^2(T)]^5}.$$

In this equation,

$$\mathcal{N}(T) \equiv \left(\frac{2\pi^2\mu(T)g^2\left\langle (F^a_{\mu\nu})^2\right\rangle_T}{N_c^2-1}\right)^2$$

contains the temperature-dependent gluon condensate $g^2\left\langle (F^a_{\mu\nu})^2\right\rangle_T$ and the inverse vacuum correlation length $\mu(T)$. We therefore obtain

$$\left\langle \mathrm{Re}\, W^{\mathrm{Mink}}_{1-\mathrm{strip}}\right\rangle =$$

$$= \exp\left[-\frac{C_R M^2(T)}{4}\int d\sigma_{13}(w)\int d\sigma_{13}(w')\int \frac{d^4p}{(2\pi)^4}\mathrm{e}^{ip(w-w')}\frac{p^2}{p^4\mathcal{K}^2(p)+M^4(T)}\right]. \qquad (26)$$

One can now reduce the 4-dimensional momentum integration to a 1-dimensional integration by using the formula

$$\int \frac{d^4p}{(2\pi)^4}\mathrm{e}^{ip(w-w')}f(|p|) = \frac{1}{4\pi^2|w-w'|}\int_0^\infty dpp^2 J_1(p|w-w'|)f(p)$$

with the J_1-Bessel function. According to Eq. (13), the product of two infinitesimal surface elements reads

$$d\sigma_{13}(w)d\sigma_{13}(w') = (\beta L_\perp)^2 d^2\xi d^2\xi'.$$

Furthermore, one can simplify the area-area correlation inside one strip ($k=0$), where the distance between the points depends only on the variable x introduced in Eq. (16):

$$|w-w'| = |\Delta w(0)| = \beta|x|\sqrt{2}.$$

Equation (26) yields the following expression:

$$\chi_0 = -\ln\left\langle \mathrm{Re}\, W^{\mathrm{Mink}}_{1-\mathrm{strip}}\right\rangle = \frac{C_R\mathcal{N}(T)M^2(T)}{16\pi^2\sqrt{2}}\beta L_\perp^2\int_{-1}^1\frac{dx}{|x|}\int_0^\infty \frac{dpp^4J_1(p\beta|x|\sqrt{2})}{p^4(p^2+\mu^2(T))^5+\mathcal{N}(T)M^4(T)}. \qquad (27)$$

The $L_\perp$-dependence of this result is consistent with the color transparency of a color-neutral dipole of size $L_\perp$ interacting with the gluon plasma. Furthermore, the x-integral in Eq. (27) does not diverge at $x=0$, since this singularity is cancelled by the Bessel function.

By using Eqs. (1), (17), and (18), we can now determine $\hat{q}$:

$$\hat{q} = -\frac{4\sqrt{2}}{L_\parallel L_\perp^2} \ln \left\langle \mathrm{Re}\, W^{\mathrm{Mink}}_{L_\parallel \times L_\perp} \right\rangle = \frac{4}{\beta L_\perp^2} \frac{1}{n} \sum_{k=0}^{n-1} (n-k)\chi_k,$$

where

$$\chi_k = \frac{C_R \mathcal{N}(T) M^2(T)}{16\pi^2} \beta L_\perp^2 \int_{-1}^{1} \frac{dx}{\sqrt{k^2+2kx+2x^2}} \int_0^\infty \frac{dp p^4 J_1(p\beta\sqrt{k^2+2kx+2x^2})}{p^4(p^2+\mu^2(T))^5 + \mathcal{N}(T)M^4(T)}.$$

Here, we have used Eq. (16) for the distance $|\Delta w(k)|$ between two points belonging to the strips separated from each other by the interval βk. Our final result reads

$$\hat{q} = \frac{C_R \mathcal{N}(T) M^2(T)}{4\pi^2 n} \sum_{k=0}^{n-1} (n-k) \int_{-1}^{1} \frac{dx}{\sqrt{k^2+2kx+2x^2}} \int_0^\infty \frac{dp p^4 J_1\left(p\beta\sqrt{k^2+2kx+2x^2}\right)}{p^4(p^2+\mu^2(T))^5 + \mathcal{N}(T)M^4(T)}. \tag{28}$$

Let us consider a gluon traversing the medium, for which R is the adjoint representation, and $C_R = N_c = 3$. Furthermore, we assume that the critical temperature $T_c = 270\,\mathrm{MeV}$ in SU(3) quenched theory [20]. The temperature behavior of $\hat{q}$ and the growth of $\hat{q}$ with T depend on the functions $g^2 \left\langle (F^a_{\mu\nu})^2 \right\rangle_T$, $\mu(T)$, and $M(T)$. To see whether this dependence is strong or not, we determine $\hat{q}(T)$ for two possible choices (I and II) of these functions.

In case I, the nonperturbative value of the thermal strong coupling $g(m_D, T)$ is fixed by self-consistency [21]: $g(m_D, T) = 2.5$. This choice defines $M(T)$ through Eq. (25) with $m_D = g(m_D, T)T$. As suggested by the *low-temperature* lattice data [11, 12], the inverse vacuum correlation length can be taken constant up to the temperature of dimensional reduction [22], $T_{\mathrm{d.r.}} \simeq 2T_c = 540\,\mathrm{MeV}$. Above this temperature, all dimensionful quantities become proportional to the corresponding power of T. Therefore, $\mu(T) = \mathrm{const}$ until $T_{\mathrm{d.r.}}$, whereas $\mu(T) \propto T$ at $T > T_{\mathrm{d.r.}}$. The proportionality coefficient in the last equation can be fixed by the continuity of $\mu(T)$ across $T_{\mathrm{d.r.}}$:

$$\mu(T) = 1.66T \quad \text{at} \quad T > T_{\mathrm{d.r.}}.$$

The temperature dependence of the chromo-magnetic condensate was calculated in Ref. [23]:

$$g^2 \left\langle (F^a_{\mu\nu})^2 \right\rangle_T = g^2 \left\langle (F^a_{\mu\nu})^2 \right\rangle \coth\left(\frac{\mu}{2T}\right) \quad \text{at} \quad T_c < T < T_{\mathrm{d.r.}}.$$

It is also nearly constant up to $T_{\mathrm{d.r.}}$. At $T > T_{\mathrm{d.r.}}$, $g^2 \left\langle (F^a_{\mu\nu})^2 \right\rangle_T \propto T^4$, and the proportionality coefficient again follows from continuity of $g^2 \left\langle (F^a_{\mu\nu})^2 \right\rangle_T$ across $T_{\mathrm{d.r.}}$:

$$g^2 \left\langle (F^a_{\mu\nu})^2 \right\rangle_T = 61.46T^4 \quad \text{at} \quad T > T_{\mathrm{d.r.}}.$$

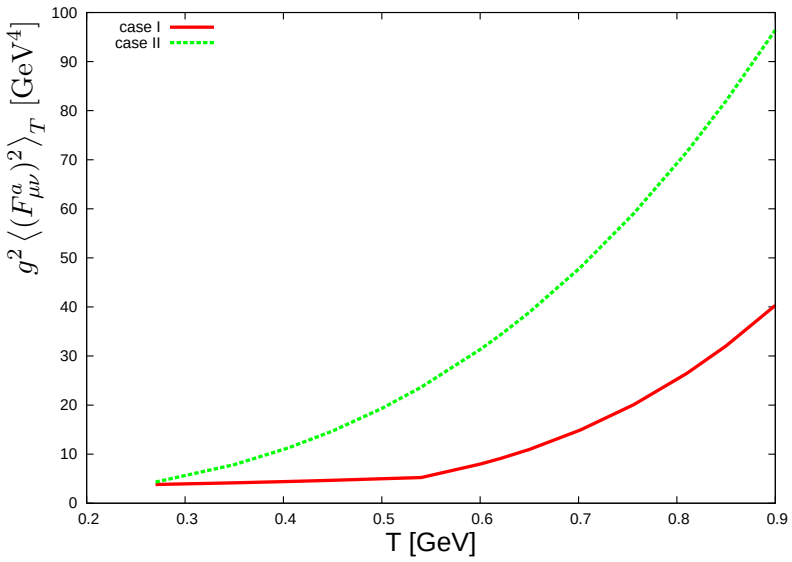


Figure 3: The chromo-magnetic condensate as a function of temperature at $T_c \leq T \leq 900\,\mathrm{MeV}$ in cases I and II.

In case II, we define the parameter $M(T)$ through the perturbative 1-loop strong coupling [22]:

$$g^{-2}(T) = 2b_0 \ln\frac{T}{\Lambda}, \quad \text{where} \quad b_0 = \frac{11N_c}{48\pi^2}\Big|_{N_c=3} = \frac{11}{16\pi^2}, \quad \Lambda \simeq 0.104T_c.$$

Furthermore, *high-temperature* lattice data [22] suggest the parametrization

$$\mu(T) = 1.04g^2(T)T,$$

where the coefficient has been fixed by the value $\mu(T_c) = \mu$. The same lattice data suggest also a temperature-dependent spatial string tension

$$\sigma(T) = [cg^2(T)T]^2, \quad \text{where} \quad c = 0.566.$$

Note that such a value of the coefficient c corresponds to a spatial string tension $\sigma(T_c) = (485\,\mathrm{MeV})^2$, that is slightly larger than the standard zero-temperature value $\sigma(0) = (440\,\mathrm{MeV})^2$. The temperature-dependent chromo-magnetic condensate can then be obtained from Eq. (5) at $N_c = 3$: $g^2\langle(F^a_{\mu\nu})^2\rangle_T = \frac{72}{\pi}\mu^2(T)\sigma(T)$. For illustration, we present the chromo-magnetic condensates for both cases I and II in Fig. 3.

Because of the much smaller density of scattering partners in the hadronic phase, typical values of $\hat{q}$ at $T < T_c$ are $\sim 0.01\,\mathrm{GeV}^2/\mathrm{fm}$, which is by two orders of magnitude smaller than

in the quark-gluon plasma [24]. For this reason, we set $\hat{q}(T) = \hat{q}(T) - \hat{q}(T_c)$, i.e. $\hat{q}(T_c) = 0$. Furthermore, we truncate $n = 10 \gg 1$ and use a small value $\zeta = 0.1 \ll 1$. We then obtain $\hat{q}$ as a function of temperature in the interval $270\,\mathrm{MeV} \leq T \leq 900\,\mathrm{MeV}$ for both cases I and II, cf. Fig. 4. Both calculations of $\hat{q}$ follow a temperature dependence $\propto T^3$. We find

$$\hat{q}(T)^{\mathrm{fit}}_{\mathrm{case\,I}} = 0.16(T/T_c)^3\,\mathrm{GeV}^2/\mathrm{fm}, \quad \hat{q}(T)^{\mathrm{fit}}_{\mathrm{case\,II}} = 0.26(T/T_c)^3\,\mathrm{GeV}^2/\mathrm{fm}.$$

These fits are inspired by Eq. (28). Indeed, counting the powers of T in this equation at high temperatures, one sees that

$$\hat{q} \propto T^3 \quad \text{at} \quad T \gtrsim T_{\mathrm{d.r.}}.$$

Furthermore, at $T = 900\,\mathrm{MeV}$ we have tested the sensitivity of our results against an increase of the number of strips n. An increase of the number of strips leads to a small increase of $\hat{q}(T)$, namely

$$\hat{q}(900\,\mathrm{MeV})^{(n=10)}_{\mathrm{case\,I}} = 1.26\,\mathrm{GeV}^2/\mathrm{fm}, \quad \hat{q}(900\,\mathrm{MeV})^{(n=50)}_{\mathrm{case\,I}} = 1.39\,\mathrm{GeV}^2/\mathrm{fm};$$

$$\hat{q}(900\,\mathrm{MeV})^{(n=10)}_{\mathrm{case\,II}} = 1.78\,\mathrm{GeV}^2/\mathrm{fm}, \quad \hat{q}(900\,\mathrm{MeV})^{(n=50)}_{\mathrm{case\,II}} = 1.98\,\mathrm{GeV}^2/\mathrm{fm}.$$

We have also addressed the dependence of $\hat{q}(T)$ on the parameter ζ, which measures the smallness of the energy of thermal gluons with respect to their characteristic spatial momenta. For small values of ζ under consideration, specifically $\zeta < \frac{1}{\sqrt{3}} \simeq 0.58$, the function $M^2(T)$, Eq. (25), describing the imaginary part of the hard thermal loop polarization operator, is a monotonically increasing function of ζ. Therefore, since $M^2(T)$ enters both the numerator and the denominator of the resulting Eq. (28), only a numerical analysis can say whether $\hat{q}(T)$ increases or decreases with the increase of ζ. We have depicted the results of such an analysis in Fig. 5 for case I and in Fig. 6 for case II. In case I, we observe a slow monotonic decrease of $\hat{q}(T)$ with the increase of ζ. In case II, we observe a small increase of $\hat{q}(T)$ when ζ varies from 0.1 to 0.3 and an essentially constant behavior of $\hat{q}(T)$ with the further increase of ζ. In both cases, the dependences of $\hat{q}(T)$ on ζ are very weak, which indicates that the predictions of our model are rather stable.

IV. CONCLUDING REMARKS

In this paper, we have evaluated the jet quenching parameter $\hat{q}$ in SU(3) YM theory. Our calculation is based on a nonperturbative approach, represented by the stochastic vacuum

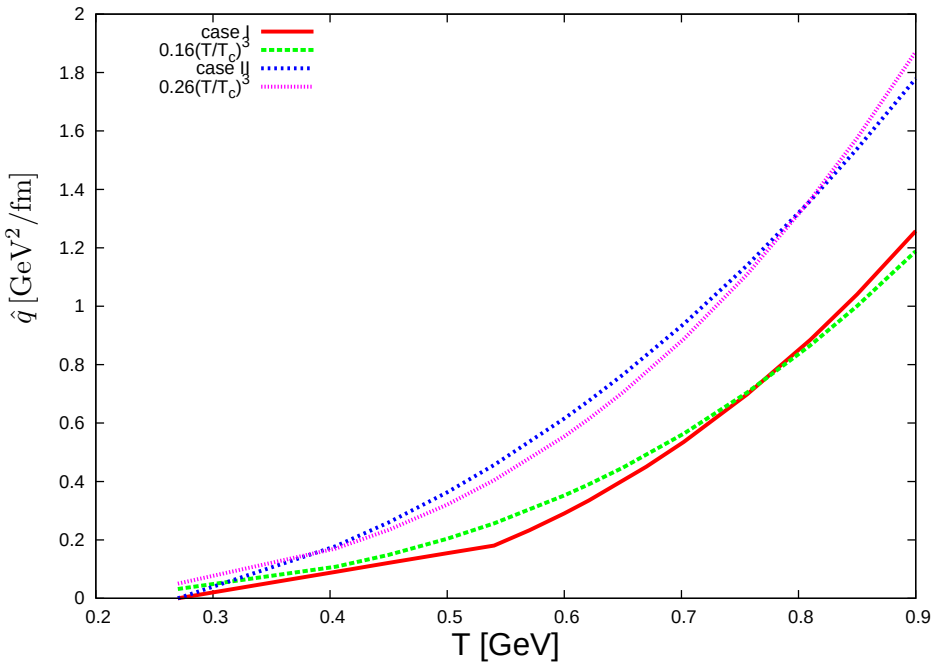


Figure 4: The jet quenching parameter $\hat{q}(T)$ in case I (lower full curve) and II (upper dashed curve), and the interpolating fitted curves $\sim T^3$ in both cases.

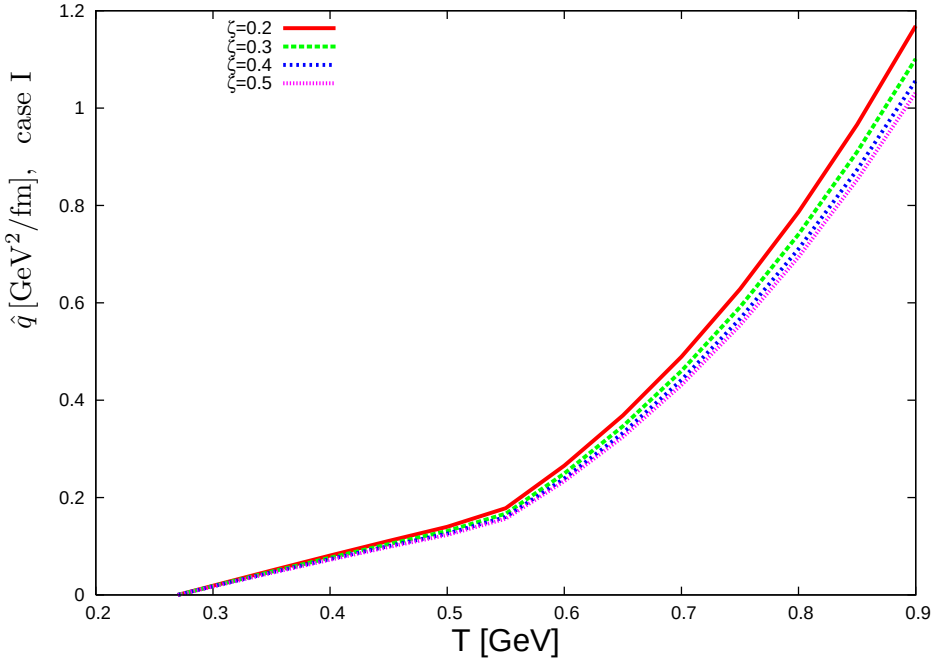


Figure 5: The jet quenching parameter $\hat{q}(T)$ in case I for various values of the parameter ζ.

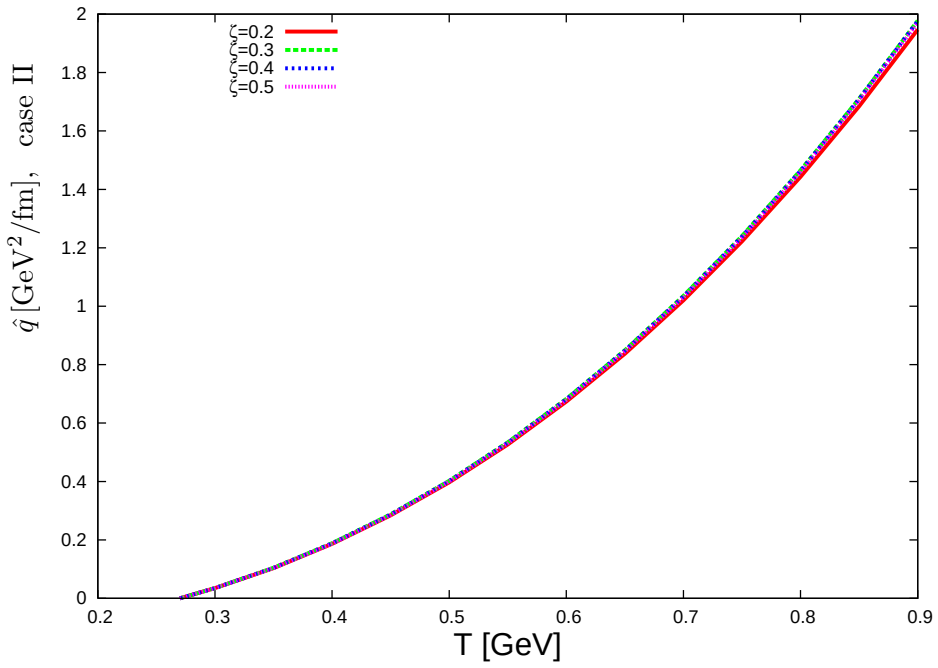


Figure 6: The jet quenching parameter $\hat{q}(T)$ in case II for various values of the parameter ζ.

model, which describes the scattering of a fast parton off a hard thermal gluon in the leading approximation $\propto (g^2 \left\langle (F^a_{\mu\nu})^2 \right\rangle_T)^2$. In our scenario of jet quenching, the gluon plasma has two components. The chromo-magnetic condensate describes the soft component of the gluon plasma, which has been called "epoxy" in the works of the Stony Brook group [25]. The hard component of the plasma (with momenta larger than the inverse vacuum correlation length) is represented in our approach by the hard thermal loop effective theory. In some sense, such a picture of a two-component gluon plasma resembles the two-component Landau model of superfluid quantum liquids [26].

In our model, jet quenching originates from Landau damping of soft gluons by the on-shell hard thermal gluons. The analytic result for $\hat{q}(T)$ is given by Eq. (28). Numerically, we have calculated $\hat{q}(T)$ for two alternative parametrizations of the chromo-magnetic condensate and the vacuum correlation length, thereby testing the stability of the result against possible uncertainties of these quantities. The numerical results are plotted in Fig. 4 along with the corresponding fitting curves. Our values of $\hat{q}$ are somewhat larger than the values obtained in pQCD, $\hat{q}_{\rm pQCD} = 1.1 \div 1.4\,{\rm GeV}^2/{\rm fm}$ [1] and closer to those of other recent nonperturbative calculations [24, 27], where $\hat{q} = 1.0 \div 1.9\,{\rm GeV}^2/{\rm fm}$. However, due to the difference of our model from that of Ref. [27], our result Eq. (28) differs parametrically from the result of

that paper.

Note finally that our values of the jet quenching parameter are close also to the effective values in $\mathcal{N} = 4$ SYM [5] corresponding to QCD. Indeed, analyzing possible matchings of the two theories, Gubser [28] has argued that the result of Ref. [5] would correspond to the values of the jet quenching parameter of a heavy quark in QCD $\hat{q} = 0.61 \div 2.6\,\mathrm{GeV}^2/\mathrm{fm}$. Since the result of Ref. [5] is not proportional to the Casimir operator C_R, the values of the jet quenching parameter for a gluon should be the same. These values are of the same order of magnitude as those obtained in the present paper.

Acknowledgments

We are grateful to D. D. Dietrich for a collaboration at the early stage of the work. The work of D.A. has been supported through the contract MEIF-CT-2005-024196.

---

[1] R. Baier, Y. L. Dokshitzer, A. H. Mueller, S. Peigne and D. Schiff, Nucl. Phys. B **483**, 291 (1997); for reviews see: R. Baier, D. Schiff and B. G. Zakharov, Ann. Rev. Nucl. Part. Sci. **50**, 37 (2000); M. Gyulassy, I. Vitev, X. N. Wang and B. W. Zhang, "Jet quenching and radiative energy loss in dense nuclear matter," arXiv:nucl-th/0302077.

[2] J. Dolejsi, J. Hüfner and B. Z. Kopeliovich, Phys. Lett. B **312**, 235 (1993).

[3] O. Nachtmann, Annals Phys. **209** (1991) 436.

[4] For a review see: S. Donnachie, H. G. Dosch, O. Nachtmann and P. Landshoff, *Pomeron physics and QCD,* Camb. Monogr. Part. Phys. Nucl. Phys. Cosmol. **19**, 1 (2002).

[5] H. Liu, K. Rajagopal and U. A. Wiedemann, Phys. Rev. Lett. **97**, 182301 (2006); JHEP **0703**, 066 (2007).

[6] H. G. Dosch, Phys. Lett. B **190**, 177 (1987); H. G. Dosch and Yu. A. Simonov, Phys. Lett. B **205**, 339 (1988); for a review see: A. Di Giacomo, H. G. Dosch, V. I. Shevchenko and Yu. A. Simonov, Phys. Rept. **372**, 319 (2002).

[7] A. I. Shoshi, F. D. Steffen and H. J. Pirner, Nucl. Phys. A **709**, 131 (2002).

[8] H. J. Pirner and N. Nurpeissov, Phys. Lett. B **595**, 379 (2004).

[9] E. Meggiolaro, Phys. Lett. B **451**, 414 (1999).

[10] A. Di Giacomo and H. Panagopoulos, Phys. Lett. **B 285**, 133 (1992).

[11] A. Di Giacomo, E. Meggiolaro and H. Panagopoulos, Nucl. Phys. B **483**, 371 (1997).

[12] M. D'Elia, A. Di Giacomo and E. Meggiolaro, Phys. Rev. D **67**, 114504 (2003).

[13] For reviews see: A. Di Giacomo, "Non perturbative QCD," arXiv:hep-lat/9912016; Czech. J. Phys. **51**, B9 (2001); "QCD vacuum and confinement," arXiv:hep-lat/0204001.

[14] G. S. Bali, N. Brambilla and A. Vairo, Phys. Lett. B **421**, 265 (1998).

[15] A. I. Shoshi, F. D. Steffen, H. G. Dosch and H. J. Pirner, Phys. Rev. D **68**, 074004 (2003).

[16] D. Antonov, D. Ebert and Yu. A. Simonov, Mod. Phys. Lett. A **11**, 1905 (1996); D. Antonov, Surveys High Energ. Phys. **14**, 265 (2000), section 2.1.

[17] For a review see: J. P. Blaizot and E. Iancu, Phys. Rept. **359**, 355 (2002).

[18] V. V. Klimov, Sov. J. Nucl. Phys. **33**, 934 (1981); Sov. Phys. JETP **55**, 199 (1982); H. A. Weldon, Phys. Rev. D **26**, 1394 (1982).

[19] A. M. Polyakov, *Gauge Fields and Strings* (Harwood Academic Publishers, Chur, 1987), chapter 2.3; see also: D. Antonov and H. J. Pirner, Eur. Phys. J. C **51**, 633 (2007).

[20] For a recent review see: P. Petreczky, Eur. Phys. J. C **43**, 51 (2005).

[21] J. Braun and H. J. Pirner, Phys. Rev. D **75**, 054031 (2007); D. Antonov, S. Domdey and H. J. Pirner, Nucl. Phys. A **789**, 357 (2007).

[22] G. S. Bali, J. Fingberg, U. M. Heller, F. Karsch and K. Schilling, Phys. Rev. Lett. **71**, 3059 (1993); F. Karsch, E. Lärmann and M. Lütgemeier, Phys. Lett. B **346**, 94 (1995); G. Boyd, J. Engels, F. Karsch, E. Lärmann, C. Legeland, M. Lütgemeier and B. Petersson, Nucl. Phys. B **469**, 419 (1996).

[23] N. O. Agasian, Phys. Lett. B **562**, 257 (2003).

[24] For a recent reference see: J. Casalderrey-Solana and X. N. Wang, Phys. Rev. C **77**, 024902 (2008).

[25] G. E. Brown, C. H. Lee, M. Rho and E. Shuryak, Nucl. Phys. A **740**, 171 (2004); G. E. Brown, L. Grandchamp, C. H. Lee and M. Rho, Phys. Rept. **391**, 353 (2004).

[26] See e.g.: E. M. Lifshitz and L. P. Pitaevskii, *Statistical Physics, Part II* (Pergamon, Oxford, 1980).

[27] A. Majumder, B. Müller and X. N. Wang, Phys. Rev. Lett. **99**, 192301 (2007).

[28] S. S. Gubser, Nucl. Phys. B **790**, 175 (2008).

[29] Throughout the paper, we use the notation $A_\mu \equiv A_\mu^a t^a$, where t^a's are the generators of the

group SU(N_c) in a given representation R. The trace "tr" is normalized by dividing over the trace of the unit matrix $\hat{1}_R$ in the representation R. Therefore, with this definition, $\mathrm{tr}\,\hat{1}_R = 1$.

[30] The normalization of the function D^B can be proven by taking the $(T \to 0)$-limit and imposing for the correlation function $\left\langle E_i^a(x) E_k^b(x') \right\rangle$ the same parametrization (11) with some other function D^E instead of D^B. Due to the unbroken $O(4)$-invariance at $T = 0$, one has $D^E(0) = D^B(0)$. On the other hand, using the parametrization (11), one has

$$\left\langle (F_{\mu\nu}^a)^2 \right\rangle = 2 \sum_{i=1}^{3} \left[\left\langle (E_i^a)^2 \right\rangle + \left\langle (B_i^a)^2 \right\rangle \right] = \frac{1}{2} \left\langle (F_{\mu\nu}^a)^2 \right\rangle \left[D^E(0) + D^B(0) \right].$$

This proves that $D^B(0) = 1$.

[31] For brevity, we use the same notations for a function or an operator and its Fourier image. What is implied in each particular case is clearly defined by the corresponding argument.